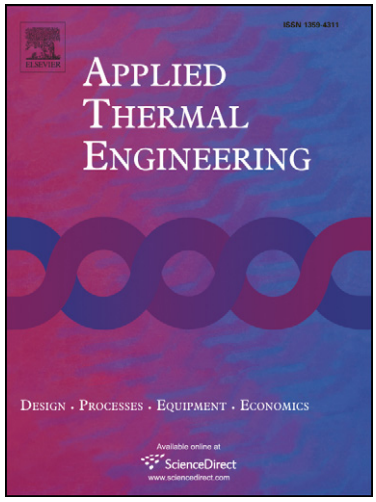

Experimental study of an ammonia-water bubble absorber using a plate heat exchanger for absorption refrigeration machines

Jesús Cerezo, Mahmoud Bourouis, Manel Vallès, Alberto Coronas, Roberto Best

PII: S1359-4311(08)00230-5
DOI: 10.1016/j.applthermaleng.2008.05.012
Reference: ATE 2516

To appear in: *Applied Thermal Engineering*

Received Date: 17 September 2007
Revised Date: 27 March 2008
Accepted Date: 13 May 2008

Please cite this article as: J. Cerezo, M. Bourouis, M. Vallès, A. Coronas, R. Best, Experimental study of an ammonia-water bubble absorber using a plate heat exchanger for absorption refrigeration machines, *Applied Thermal Engineering* (2008), doi: 10.1016/j.applthermaleng.2008.05.012

EXPERIMENTAL STUDY OF AN AMMONIA-WATER BUBBLE ABSORBER USING A PLATE HEAT EXCHANGER FOR ABSORPTION REFRIGERATION MACHINES

Jesús Cerezo[a], Mahmoud Bourouis[a]*, Manel Vallès[a], Alberto Coronas[a], Roberto Best[b].

[a]CREVER - Universitat Rovira i Virgili, Av. Països Catalans No. 26, 43007, Tarragona, Spain

[b]Centro de Investigación en Energía-Universidad Nacional Autónoma de México, Apto. Postal 34, Temixco 62580 Morelos, México

* Contact: Tel: +34-977 55 86 13; fax: +34-977 55 96 91

E-mail address: mahmoud.bourouis@urv.net (M. Bourouis)

ABSTRACT

The development of absorption chillers activated by renewable heat sources has increased due mainly to the increase in primary energy consumption that causes problems such as greenhouse gases and air pollution amongst others. These machines, which could be a good substitute for compression systems, could be used in the residential and food sectors which require a great variety of refrigeration conditions. Nevertheless, the low efficiency of these machines makes it necessary to enhance heat and mass transfer processes in the critical components, mainly the absorber, in order to reduce their large size.

This study used ammonia-water as the working fluid to look at how absorption takes place in a plate heat exchanger operating under typical conditions of absorption chillers, driven by low temperature heat sources. Experiments were carried out using a corrugated plate heat exchanger model NB51, with three channels, where ammonia

vapor was injected in bubble mode into the solution in the central channel. The results achieved for the absorption flux were in the range of 0.0025 - 0.0063 kg m^{-2} s^{-1}, the solution heat transfer coefficient varied between 2.7 and 5.4 kW m^{-2} K^{-1}, the absorber thermal load from 0.5 to 1.3 kW. In addition, the effect of the absorber operating conditions on the most significant efficiency parameters was analyzed. The increase in pressure, solution and cooling flow rates positively affect the absorber performance, on the other hand an increase in the concentration, cooling and solution temperature negatively affects the absorber performance.

Keywords: absorption refrigeration; absorber; bubble; plate heat exchanger; ammonia-water

Nomenclature

A	Heat transfer area, m^2
Cp	Heat capacity, kJ kg^{-1} K^{-1}
F_{AB}	Mass absorption flux, kg_{NH3} m^{-2} s^{-1}
H	Enthalpy, kW
h	Heat transfer coefficient, kW m^{-2} s^{-1}
K_m	Mass transfer coefficient, m s^{-1}
k_W	Thermal conductivity, kW m^{-1} s^{-1}
m	Mass flow rate, kg s^{-1}
Nu	Nusselt number
P	Pressure, bar
Pr	Prandtl number

Q	Heat, kW
Re	Reynolds number
T	Temperature, °C
v	Velocity, m s^{-1}
x	Ammonia concentration, % by weight

Greek symbols

δ	Plate thickness

Subscripts

AB	Absorber
C	Cooling water
EQ	Equilibrium
IN	Input
NH3	Ammonia
OUT	Output
S	Solution
SUB	Subcooling
W	Wall

1. INTRODUCTION

In recent years, energy and environmental world problems have increased interest in the development of absorption chillers driven by low temperature heat sources such as solar

thermal energy or waste heat, because they can help mitigate primary energy consumption and CO_2 emissions [1]. Development of these machines requires high efficiency in the heat and mass transfer processes which take place in the absorber, which in turn is the most important component in these systems [2]. Absorption systems can also be used in the field of refrigeration, where they could compete with compression technology in some applications. In this case, the ammonia-water mixture is the only working fluid able to produce cold down to -10°C. Also due to the use of cogeneration systems with turbine and gas engines in industrial sectors, interest has increased in cooling machines which use residual heat.

The bubble flow configuration has been recommended for the absorber due to the heat and mass transfer enhancement between the vapor and liquid phases; this is a simpler vapor distributor when compared with distributors for falling film absorbers, although it does not dissipate heat as effectively. Many researchers have reported studies on the bubble absorption processes with different geometries and working conditions, calculating the most important efficiency parameters such as the heat and mass transfer coefficients, and heat load, amongst others [3-9]. Ferreira et al. [9] developed a mathematical model for calculating the mass transfer coefficient as a function of the Reynolds and Schmidt numbers based on actual data obtained in an experimental absorber with vertical tubes which was operating at typical conditions for refrigeration. Lee et al. [4] analyzed an absorber using a flat plate heat exchanger; they concluded that the increase of solution flow rate slightly affected mass transfer, but improved heat transfer. Heat transfer was improved when gas flow rate was increased. These authors proposed an experimental correlation for the dimensionless Nusselt and Sherwood numbers.

Using plate heat exchangers in the main components of absorption refrigeration machines could reduce their size and the charge of ammonia in them, as well as improving the heat and mass transfer processes. The study will look at the absorption of ammonia in the binary mixture ammonia-water using a plate heat exchanger operating under typical conditions of absorption chillers driven by low temperature heat sources. A sensitivity study was done using an experimental set-up which varied the main operating conditions of the absorber such as pressure, temperature, concentration, and mass flow rate of the ammonia-water solution, and the temperature and mass flow rate of the cooling water. The efficiency parameters calculated were the heat and mass transfer coefficients, thermal load, and the degree of subcooling in the solution leaving the absorber.

This study was part of a research project funded by the Spanish Ministry of Education and Science and Education which dealt with the technological development of the absorber and generator for absorption refrigeration machines using plate heat exchangers [10].

2. Description of the experimental set-up

The experimental equipment was designed to study the absorption process in a channel of a plate heat exchanger in a wide range of the different operating conditions; the equipment consisted of three circuits: the NH_3-H_2O solution circuit, the cooling water circuit and the heating water circuit, as shown in figure 1.

The *NH_3-H_2O solution circuit* (black line) is where the absorption process took place in the test section. It consisted of the absorber (ABS), two stainless steel tanks (TS and

TA), a magnetic coupling gear pump, a heat exchanger (HX1), and a vapor-liquid separator (SVL). Poor solution that was previously preheated in the heat exchanger (HX1) was pumped from the storage tank (TS) to the bottom side of the absorber (ABS), where it absorbed ammonia vapor fed from an ammonia bottle, and was cooled by the *cooling water circuit*. Solution mixture and ammonia vapor flowed in co-current in the central channel, and cooling water flowed in countercurrent in both sides of the channel. Ammonia vapor was injected in bubble mode by a thin tube of 1.7 mm internal diameter from an ammonia bottle as shown in figure 2. Then, the strong solution left the absorber at the top and flowed to the vapor-liquid separator (SVL), where the vapor not absorbed was separated from the liquid phase, which was stored in the tank TA. The absorber pressure was controlled by the amount of injected vapor.

The *cooling water circuit* (blue line) consisted of a 5 kW heater (HX3), a magnetic flowmeter (F), a pump, and a heat exchanger (HX4). The flow of the cooling water and solution streams could be arranged in a co or counter current configuration. The *heating water circuit* (red line) allowed the ammonia-water solution to be preheated to a set temperature before entering the absorber. This circuit consisted of a 5 kW heater (HX2), a pump, a flowmeter, and a heat exchanger (HX1).

2.1. Absorber

Several researchers [3, 4, 11] have recommended plate heat exchangers for the main components of ammonia-water absorption systems in order to enhance heat and mass transfer processes. The absorber used in the experimental set-up was a corrugated plate heat exchanger; model NB51, type L with three channels of 0.1 m^2 effective surface area in the central channel.

2.2. Experimental measurements

The experimental variables measured in the test section were:

- Inlet and outlet temperatures of the ammonia-water solution in the plate heat exchanger;
- Inlet and outlet temperatures of cooling water temperature in the plate heat exchanger;
- Pressure at the inlet and outlet of the plate heat exchanger;
- Density, temperature, and mass flow rate of the strong and weak ammonia-water solutions;
- Mass flow rate of cooling water.

RTD temperature sensors (T) and pressure transmitters (P) were used to register the temperature in the points shown in figure 1. Coriolis flowmeters (C) were used to measure the density and flow rate of the weak and strong ammonia-water solutions. Table 1 shows the parameters measured and the corresponding accuracy for each instrument.

The thermodynamic properties of ammonia vapor entering the absorber were calculated considering the solution vapor pressure at the bottom of the absorber and equilibrium conditions.

3. Data reduction

The following parameters were selected to assess the absorber performance: the *mass absorption flux, the absorber thermal load, the overall heat transfer coefficient*, and the *degree of subcooling* in the solution leaving the absorber.

The *Mass absorption flux* is the absorbed mass flow rate per unit of heat transfer area and it is expressed by the following equation:

$$F_{AB} = \frac{m_{NH3}}{A} \tag{1}$$

The *Absorber thermal load* is defined as the heat released in the absorber which is removed by cooling water and is calculated as:

$$Q_{AB} = m_C Cp_C (T_{C,OUT} - T_{C,IN}) \tag{2}$$

$$Q_{AB} = UA\Delta T_{ML,EQ} \tag{3}$$

The *overall heat transfer coefficient* (U) is given by:

$$U = \frac{Q_{AB}}{A\Delta T_{ML,EQ}} \tag{4}$$

U is also defined as follows as the sum of the thermal resistances:

$$U = \frac{1}{1/h_C + \delta/k_W + 1/h_S} \tag{5}$$

It was not possible to use the conventional *log mean temperature* (6) in some experiments, because the outlet cooling water temperature was higher than the inlet solution temperature due to the heat of absorption and the subcooling of the solution entering the absorber. In this case the *logarithmic mean temperature difference* ($\Delta T_{ML,EQ}$) defined by equation (7) was used to represent the heat transfer between solution and cooling water, in which the inlet and outlet solution temperatures are calculated at equilibrium conditions [12], eliminating subcooling conditions.

$$\Delta T_{ML} = \frac{(T_{S,IN} - T_{C,OUT}) - (T_{S,OUT} - T_{C,IN})}{Ln\dfrac{(T_{S,IN} - T_{C,OUT})}{(T_{S,OUT} - T_{C,IN})}} \tag{6}$$

$$\Delta T_{LM,EQ} = \frac{(T_{S,EQ,IN} - T_{C,OUT}) - (T_{S,EQ,OUT} - T_{C,IN})}{Ln\dfrac{(T_{S,EQ,IN} - T_{C,OUT})}{(T_{S,EQ,OUT} - T_{C,IN})}} \quad (7)$$

The *mass heat transfer coefficient* was calculated applying the same concept as for the overall heat transfer coefficient and is expressed as follows:

$$K_m = \frac{m_{NH3}}{A\Delta x_{LM}} \quad (8)$$

Δx_{LM} expresses the difference between input and output concentration and their respective equilibrium conditions:

$$\Delta x_{LM} = \frac{(x_{S,EQ,IN}\rho_{S,EQ,IN} - x_{S,IN}\rho_{S,IN}) - (x_{S,EQ,OUT}\rho_{S,EQ,OUT} - x_{S,OUT}\rho_{S,OUT})}{Ln\dfrac{(x_{S,EQ,IN}\rho_{S,EQ,IN} - x_{S,IN}\rho_{S,IN})}{(x_{S,EQ,OUT}\rho_{S,EQ,OUT} - x_{S,OUT}\rho_{S,OUT})}} \quad (9)$$

The *degree of subcooling* in the solution leaving the absorber is equal to difference between the actual outlet solution temperature and the equilibrium solution temperature at the absorber pressure and the actual outlet solution concentration:

$$\Delta T_{SUB} = T_{S,EQ,OUT} - T_{S,OUT} \quad (10)$$

4. Results

This section contains the main results regarding the determination of the water-side heat transfer coefficient, as well as the sensitivity study of the absorber performance parameters versus the main operating conditions.

4.1. Convective heat transfer coefficient on the water side

Previously, experiments were carried out introducing water in both cold and hot sides of the channels in order to calculate the *cooling water heat transfer coefficient*. From this, using the methodology reported in reference [13], two correlations were obtained as a function of the Reynolds and Prandtl numbers for the transition and turbulent zones (Eqs. (11) and (12)).

Transition zone

$$Nu_C = 0.990\,\mathrm{Re}^{0.530}\,\mathrm{Pr}^{0.330} \quad (11)$$

Turbulence zone

$$Nu_C = 0.339\,\mathrm{Re}^{0.703}\,\mathrm{Pr}^{0.330} \quad (12)$$

Figure 3 shows that the Nusselt number increases from 15.4 to 39.4 in the transition zone when the Reynolds number varies from 66 to 400, while the Nusselt number increases linearly from 38.5 to 67.8 in the turbulence zone when the Reynolds number varies between 400 and 900.

4.2. Sensitivity study with ammonia-water

The sensitivity study with ammonia-water was carried out by varying the absorber operating conditions in the intervals shown in table 2. These conditions were established from a thermodynamic simulation of a single-effect absorption cycle. The results presented below show the effect of the solution concentration and flow rate, cooling water temperature and flow rate, and pressure on the absorber performance parameters.

4.2.1. Effect of the solution flow rate and concentration

Figure 4 shows the solution heat transfer coefficient (h_S) as a function of the solution Reynolds number at different concentrations of the solution entering the absorber. When the solution Reynolds number increases, the solution heat transfer coefficient increases

almost linearly from 2.8 to 4.1 kW m^{-2} K^{-1} at a fixed inlet concentration of 33% wt. This improvement is due to a decrease in the thermal layer on the plate wall which is caused by an increase in turbulence on the solution side. On the other hand, when the inlet solution concentration decreases from 33 to 29% wt, h_S increases from 3.8 to 5.0 kW m^{-2} K^{-1} at a Re value of 290, which represents an improvement of about 25.5%. This can be explained by the increase of the driving concentration at the absorber entrance.

Figure 5 shows that the increase of the solution Reynolds number from 170 to 350 slightly affects the absorption flux, which remains almost constant at 0.0027 kg m^{-2} s^{-1} for a solution concentration of 33% wt. However; the absorption flux was increased from 0.0049 to 0.0063 kg m^{-2} s^{-1} at a concentration of 29% wt. The decrease of x_{IN} from 33 to 29 % wt improves the mass absorption flux, which varies from 0.0027 to 0.0063 kg m^{-2} s^{-1} at a Re value of 290, this being the increase for the whole working range around 90 %.

The effect of the solution flow rate on the absorber thermal load is shown in Figure 6. When the solution Reynolds number varies from 170 to 370 the absorber thermal load increases from 0.56 to 0.76 kW at a solution concentration of 33 % wt. Moreover, when the solution concentration is reduced from 33 to 29 % wt the absorber thermal load increases by around 91 % at a Re value of 290.

4.2.2. Effect of the cooling water temperature

The effect of the cooling water temperature on the absorber thermal load and the heat transfer coefficient is shown in Figure 7 (a-b respectively). The absorber thermal load increases by almost 120 % when the cooling temperature is decreased from 35 to 30 °C. The effect on the solution heat transfer coefficient is less pronounced because the log

mean temperature difference at inlet cooling water temperature of 30 ºC is much higher than at 35 °C.

4.2.3. Effect of the absorber pressure

Figure 8 (a-b) shows the absorber pressure effect on the solution heat transfer coefficient and mass absorption flux respectively. When pressure is increased from 1.6 to 2.0 bar, the solution heat transfer coefficient increases from 2.8 to 4.0 kW m^{-2} K^{-1} at the low Reynolds number Re of 170; and between 4.1 and 5.3 kW m^{-2} K^{-1} at a Re value of 350. This enhancement of the solution heat transfer coefficient is due to the increase of the pressure gradient between the interface and the vapor phase. The mass absorption flux has an almost constant value of about 0.0027 kg/m^2 s at 1.6 bar and 0.0050 kg m^{-2} s^{-1} at 2 bar, which represents an increase of around 85 %.

4.2.4. Effect of the inlet solution temperature

Inlet solution temperature slightly affects the solution heat transfer coefficient and mass absorption flux when it is varied between 38 and 42 ºC, as can be observed in Figure 9 (a-b respectively). While the heat transfer coefficient varies between 3.4 and 5.4 kW m^{-2} K^{-1}, the mass absorption flux remains almost constant at 0.0054 kg m^{-2} s^{-1} from 165 to 420 Reynolds number for both solution temperatures.

4.2.5. Effect of the cooling water flow rate

Figure 10 (a-b) shows the solution heat transfer coefficient and absorption flux as a function of the cooling water Reynolds number at solution mass flow rate of 30 and 40 kg h^{-1}. The heat transfer coefficient remains almost constant between 4.2 and 4.7 kW m^{-2} K^{-1} for both values of the solution flow rate, while the mass absorption flux increases

linearly from 0.0038 to 0.0055 kg m^{-2} s^{-1} when the solution Reynolds number is varied from 270 to 550 for both flow rates.

Similarly, the effect of the cooling water flow rate on the mass transfer coefficient and the sub-cooling of the solution leaving the absorber are shown in Figure 11 (a-b respectively). The mass transfer coefficient slowly increases from 0.001 to 0.002 m s^{-1} as the cooling water Reynolds number increases, while the degree of sub-cooling remains very low due to the fact that the absorber was operated at almost the maximum mass absorption flux.

5. Conclusions

This study used ammonia-water as the working fluid to look at how absorption takes place in a channel of a plate heat exchanger operating under typical conditions of absorption chillers, driven by low temperature heat sources. The most significant results obtained are summarized below:

1. The mass absorption flux was in the range 0.0025 - 0.0063 kg m^{-2} s^{-1}, the solution heat transfer coefficient varied between 2.7 and 5.4 kW m^{-2} K^{-1}, the absorber thermal load from 0.5 to 1.3 kW, and the mass transfer coefficient was between 0.001 and 0.002 m s^{-1}.
2. The increase of the cooling water flow rate increased the mass absorption flux, while the effect on the solution heat transfer coefficient was less pronounced. On the other hand, the solution heat transfer coefficient improved as the solution flow rate increased.

3. The mass absorption flux and solution heat transfer were improved when the absorber pressure was increased, while the increase of the solution concentration, and the cooling and solution temperatures had the opposite effect.

4. The subcooling of the solution leaving the absorber was very low, which means that almost all the potential of the plate heat exchanger to absorb ammonia vapor was used; or in other words the absorber area was entirely used to perform the absorption process.

Acknowledgements

The authors gratefully acknowledge the Spanish Ministry of Education and Science for its financial support (DPI2002-04536-C01), and Alfa Laval for providing the plate heat exchanger.

References

[1] Bourouis, M., Bruno J.C., Coronas A., Avances en equipos de absorción para aire acondicionado, in: Avances en Ingeniería de Climatización y Refrigeración, International workshop, Trodesillas-Valladolid-Spain, 15-16 de diciembre, 2005, pp. 99-113.

[2] Selim, A.M., Elsayed M. M., Performance of a packed bed absorber for water ammonia absorption refrigeration system, International Journal of Refrigeration 22 (1999) 283-292.

[3] Kang, Y.T., Christensen R.N., Kashiwagi T., Ammonia–wate bubble absorber with a plate heat exchanger, ASHRAE Trans. 104 (1998) 1-11.

[4] Lee, K.B., Chung B.H., Lee J.C., Lee C.H. and Kim S.H., Experimental analysis bubble mode in a plate-type absorber, Chem. Enginnering Sc. 57 (2002) 1923-1929.

[5] Fernandez-Seara, J., Sieres J., Rodríguez C. and Vázquez M., Ammonia-water absorption in vertical tubular absorber, International Journal of Thermal Sciences 44 (2005) 277-288.

[6] Infante Ferreira, C.A. Vertical tubular absorbers for ammonia-salt absorption refrigeration, Ph. D. Thesis, Technical University of Delft, Holland, 1985.

[7] Kang, Y.T., Nagano T., Kashiwagi T., Mass transfer correlation of NH_3-H_2O bubble absorption, International Journal of Refrigeration 25 (2002) 878-886.

[8] Kim, J-K., Jung J.Y., Kang Y.T., The effect of nano-particles on the bubble absorption performance in a binary nanofluid, International Journal of Refrigeration 29 (2006) 22-29.

[9] Infante Ferreira C.A., Keizer C. and Machilsen C.H.M., Heat and mass transfer in vertical tubular bubble absorbers for ammonia-water absorption refrigeration systems, Interational Journal of Refrigeration 7 (1984) 348-357.

[10] Desarrollo de componentes avanzados para el diseño y fabricación de máquinas de refrigeración por absorción con NH3-H2O de pequeña potencia y activación a baja temperatura. R&D Project funded by the Spanish Ministery of Science and Education, DPI2002-04536-C01, 2003.

[11] Christensen, R.N., Y.T. Kang, S. Garimella, D. Priedeman, Generator absorber heat exchange (GAX) cycle modeling, component design and tests, Final Report to LG Electronics, Contract number: 862805-01/ 062805, 1996.

[12] Cerezo J., Estudio del proceso de absorción con amoníaco-agua en intercambiadores de placas para equipos de refrigeración por absorción, Ph. D. Thesis, Rovira i Virgili University of Tarragona, Spain, 2006.

[13] Kakaç S., Liu H., heat exchangers: selection, rating, and thermal design. Boca Raton, Florida,CRC, c1998.

CAPTION LEGENDS

Fig. 1. Schematic diagram of the experimental set-up.

Fig. 2. Injection of vapor in the absorber.

Fig. 3. Effect of flow rate on the Nusselt number for cooling water at transition and turbulence zone.

Fig. 4. Effect of solution Reynolds number and concentration on the solution heat transfer coefficient.

Fig. 5. Effect of solution Reynolds number and concentration on the mass absorption flux.

Fig. 6. Effect of solution Reynolds number on the absorber thermal load.

Fig. 7. Effect of cooling water temperature on the (a) absorber thermal load and (b) heat transfer coefficient.

Fig. 8. Effect of the absorber pressure on (a) the solution heat transfer coefficient, and (b) mass absorption flux.

Fig. 9. Effect of the inlet solution concentration on (a) the solution heat transfer coefficient, (b) and mass absorption flux.

Fig. 10. Effect of cooling water flow rate on (a) the solution heat transfer coefficient, and (b) mass absorption flux.

Fig. 11. Effect of the cooling flow rate on (a) the overall mass transfer coefficient, and (b) degree of subcooling of the solution leaving the absorber.

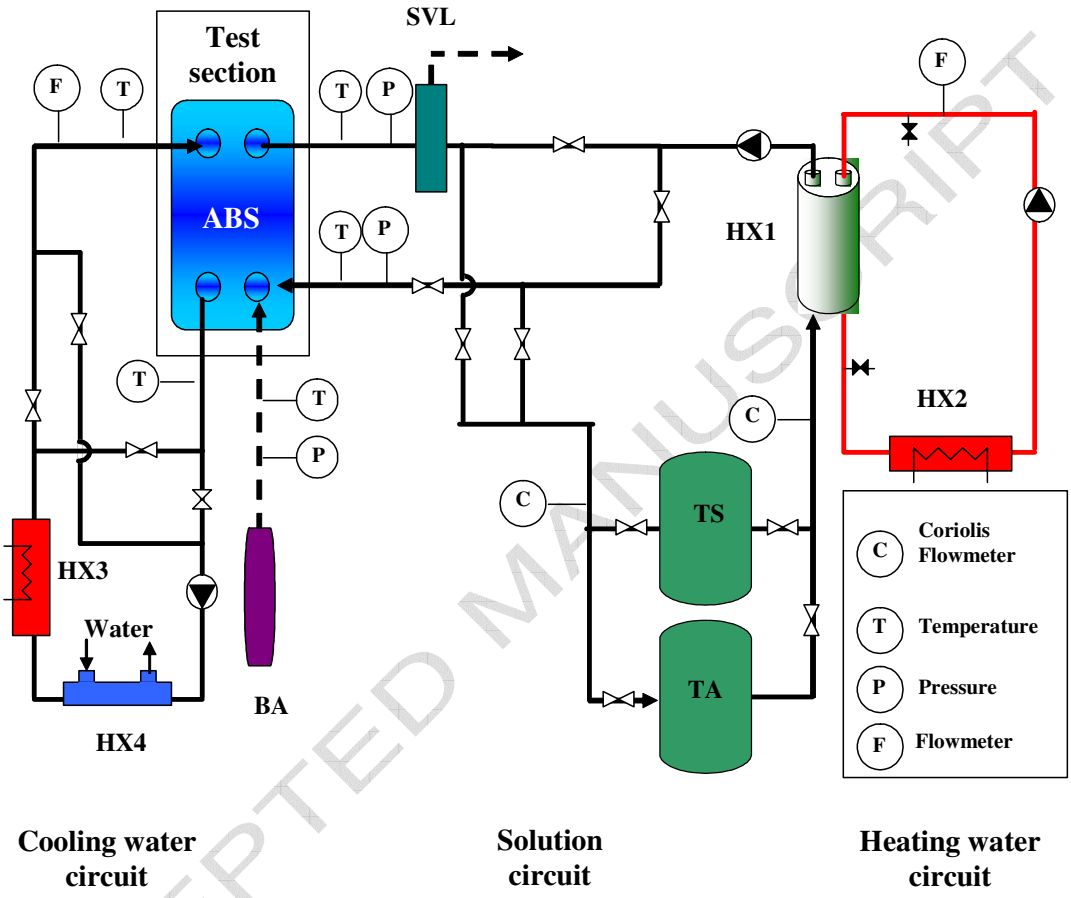

Fig. 1. Schematic diagram of the experimental set-up.

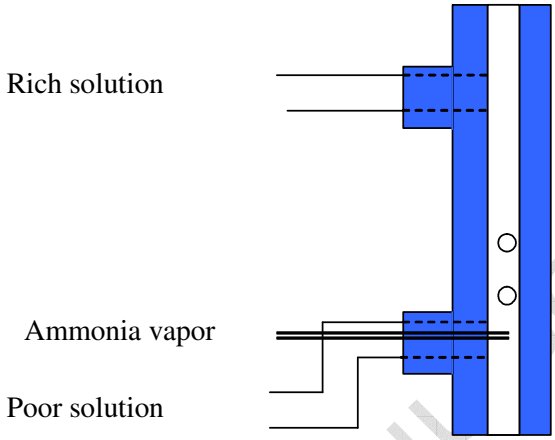

Fig. 2. Injection of vapor in the absorber.

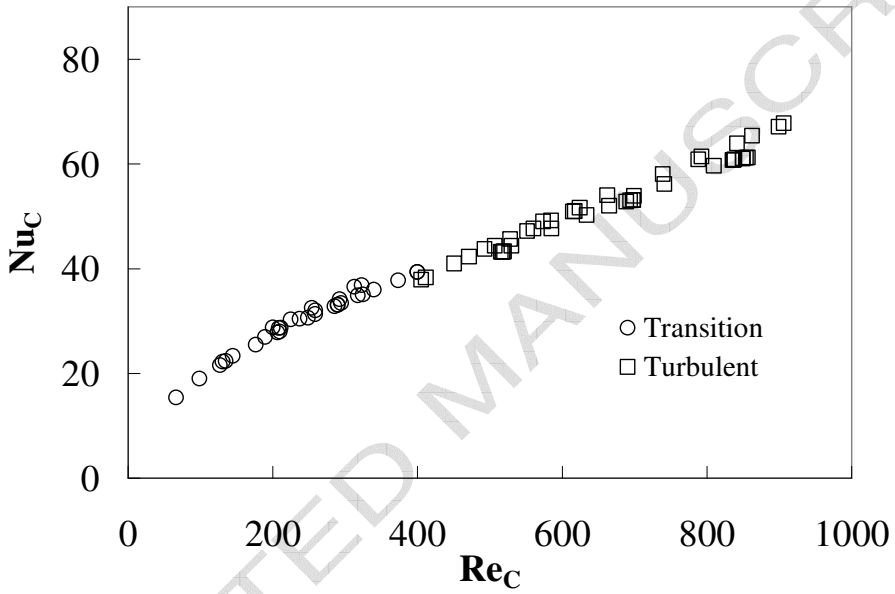

Fig. 3. Effect of flow rate on the Nusselt number for cooling water at transition and turbulence zone.

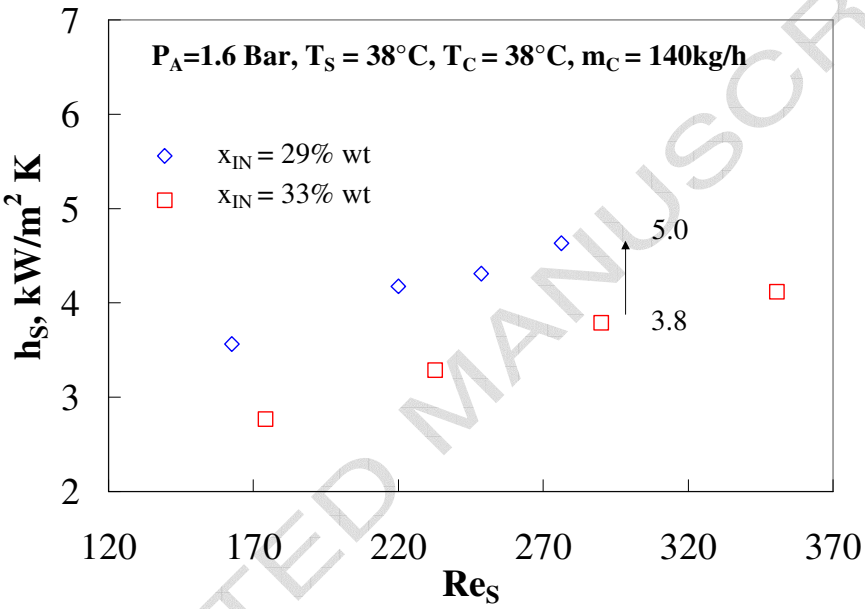

Fig. 4. Effect of solution Reynolds number and concentration on the solution heat transfer coefficient.

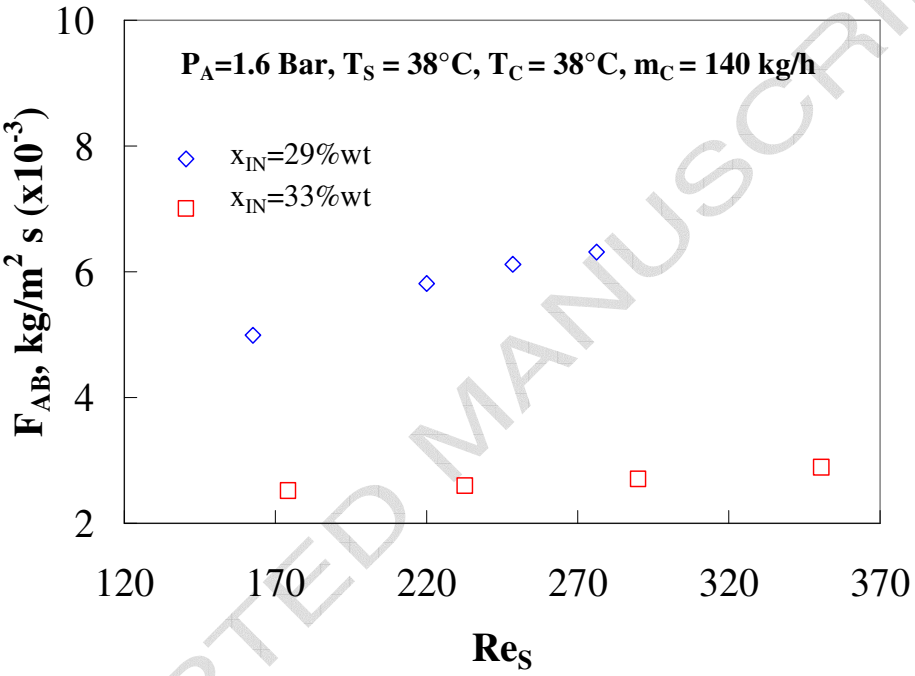

Fig. 5. Effect of solution Reynolds number and concentration on the mass absorption flux.

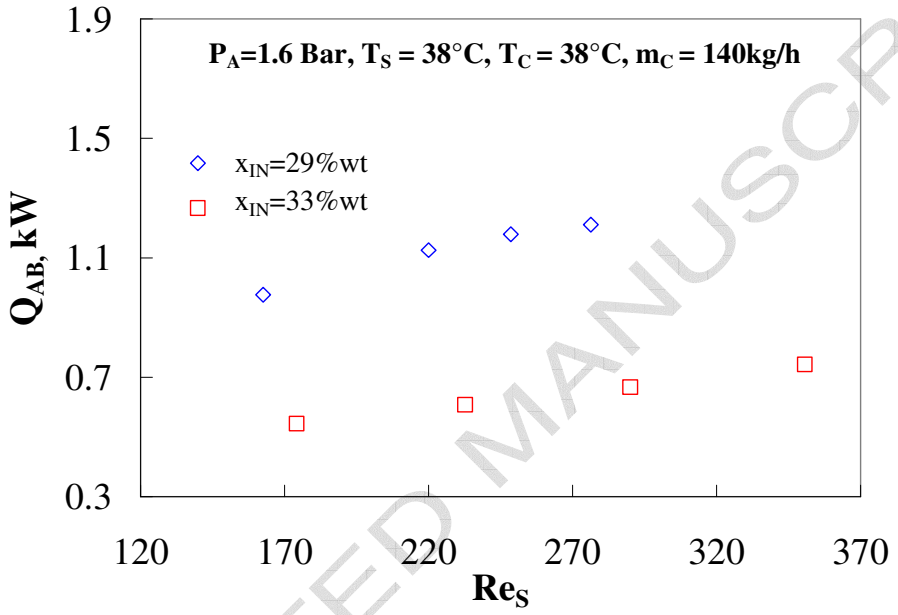

Fig. 6. Effect of solution Reynolds number on the absorber thermal load.

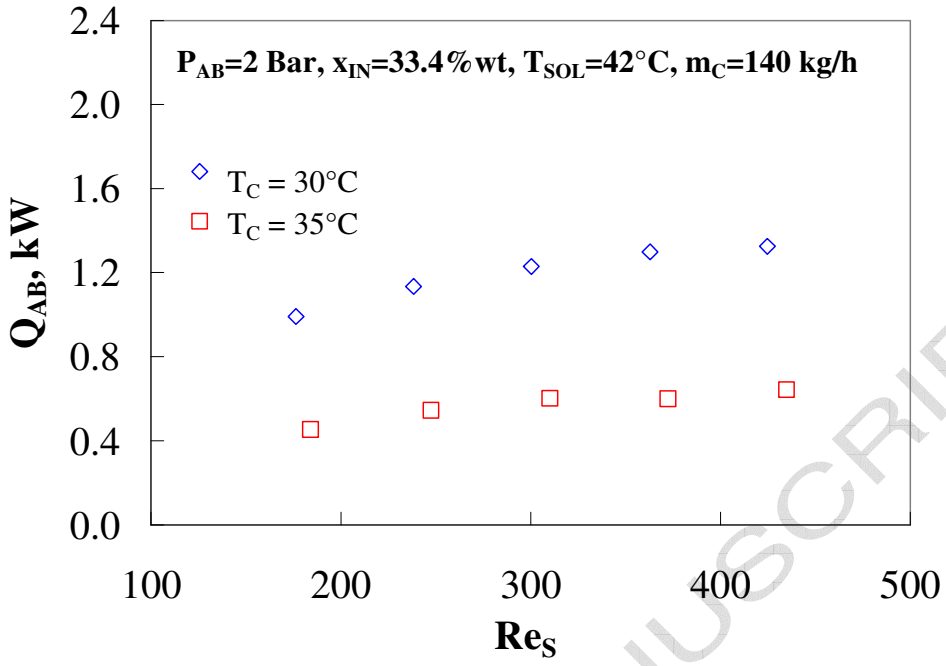

(a)

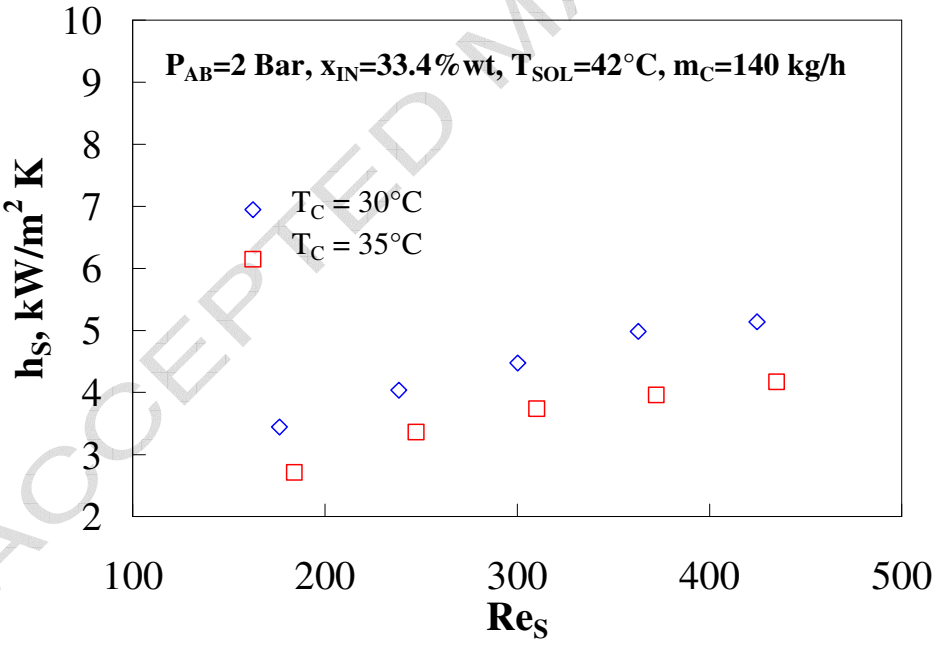

(b)

Fig. 7. Effect of cooling water temperature on the (a) absorber thermal load and (b) heat transfer coefficient.

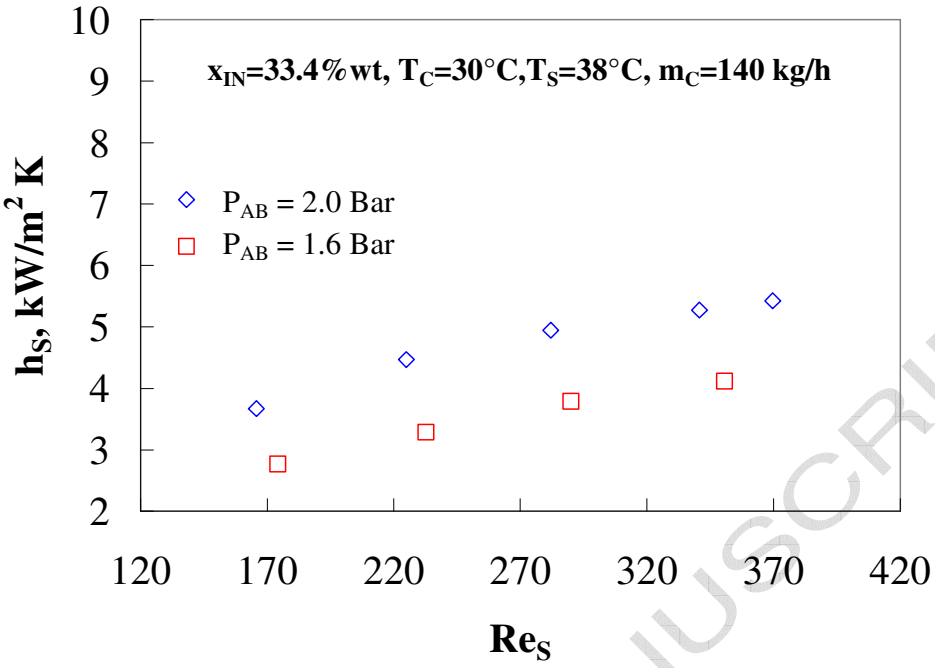

(a)

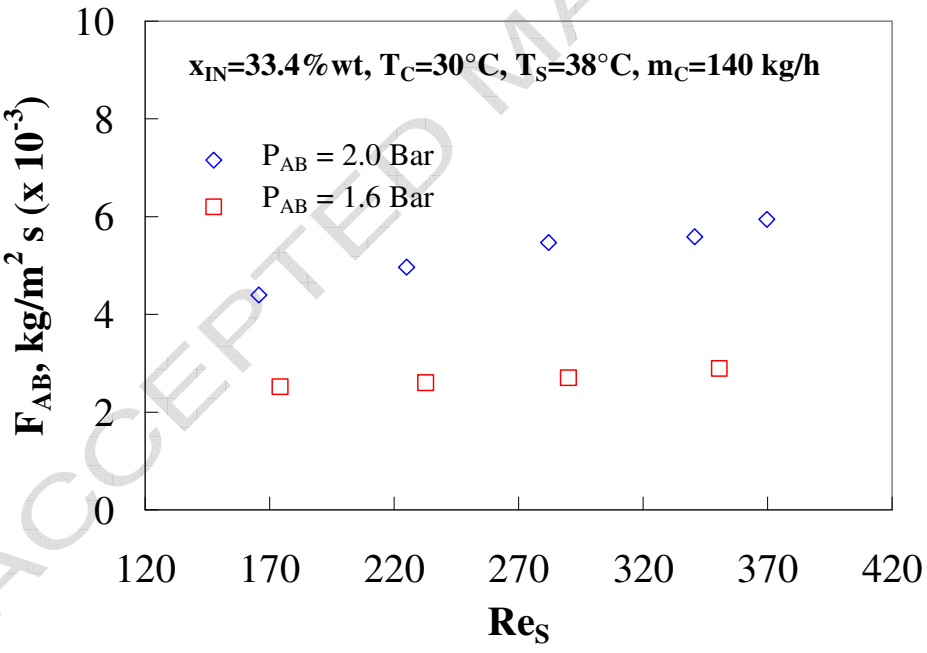

(b)

Fig. 8. Effect of the absorber pressure on (a) the solution heat transfer coefficient, and (b) mass absorption flux.

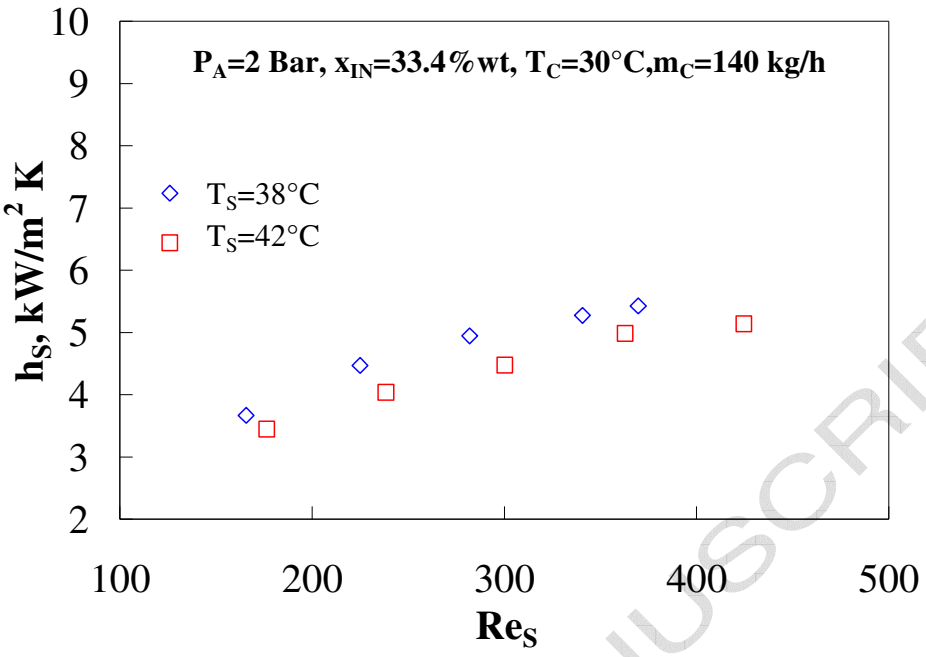

(a)

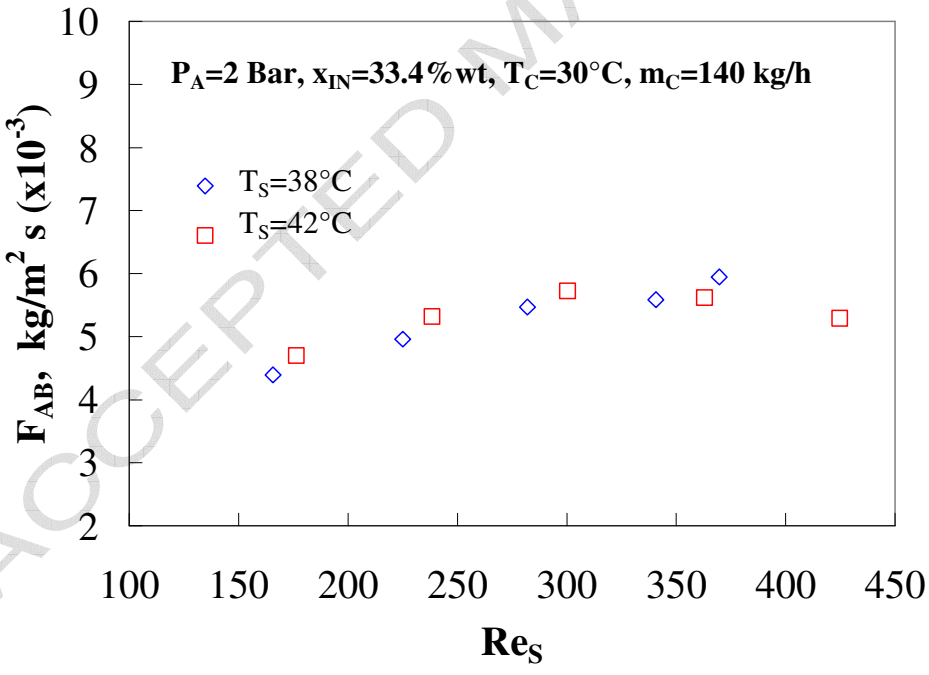

(b)

Fig. 9. Effect of the inlet solution concentration on (a) the solution heat transfer coefficient, (b) and mass absorption flux.

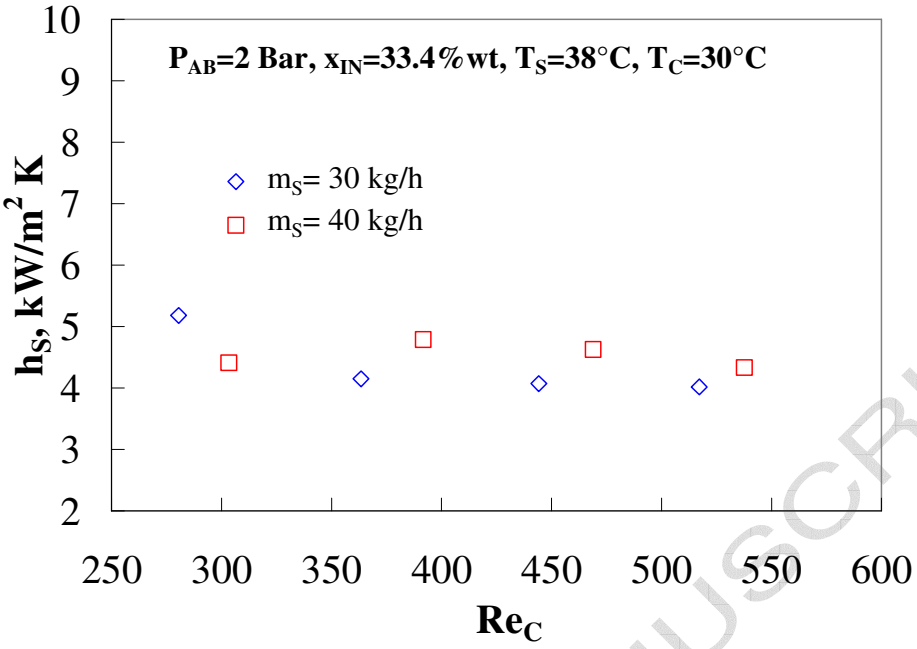

(a)

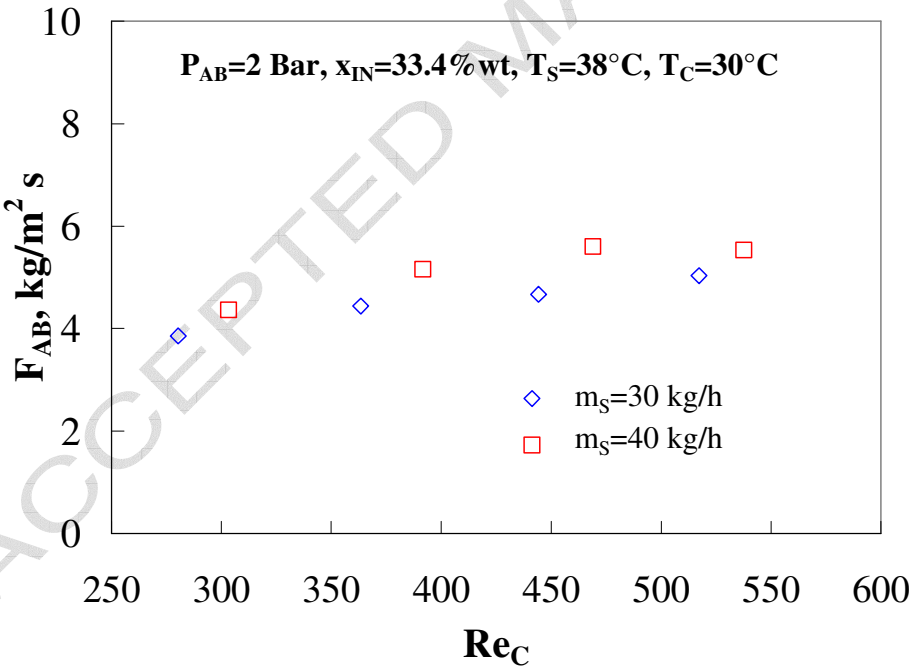

(b)

Fig. 10. Effect of cooling water flow rate on (a) the solution heat transfer coefficient, and (b) mass absorption flux.

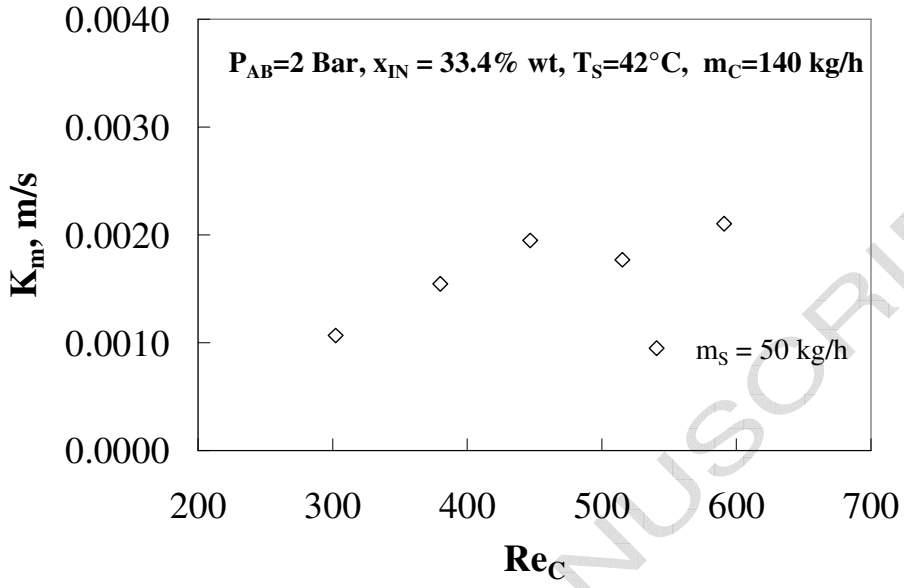

(a)

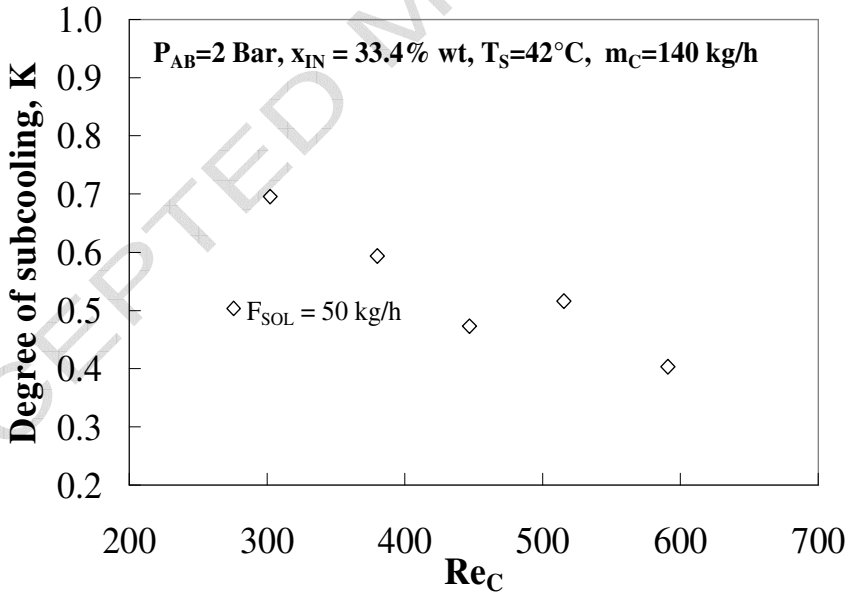

(b)

Fig. 11. Effect of the cooling flow rate on (a) the overall mass transfer coefficient, and (b) degree of subcooling of the solution leaving the absorber.

Table 1
Measured variable and accuracy of the instruments

Name	Instrumentation	Variable measured	Accuracy
C	Coriolis flowmeter	Density Solution flow rate	± 0.2, kg m^{-3} ± 0.05% of flow rate
F	Cooling flowmeter	Water flow rate	± 0.25% of flow rate
P	Pressure Gauge	Pressure	± 0.02, bar
T	PT100	Temperature	± 0.1, K

Table 2
Absorber operating conditions

Parameter	Range
Outlet solution temperature (°C)	30 - 40
Vapor temperature (°C)	-8 - 0
Inlet solution temperature (°C)	35 - 55
Inlet solution concentration (NH_3 mass fraction)	0.30 - 0.38
Outlet solution concentration (NH_3 mass fraction)	0.31 - 0.42